

# High-temperature deformation of cordierite glass-ceramic/SiC platelet composites

R. CHAIM

*Department of Materials Engineering, Technion-Israel Institute of Technology, Haifa, 32000 Israel*

A. MUNOZ, H. MIRANDA, A. DOMINGUEZ-RODRIGUEZ

*Departamento de Física de la Materia Condensada, Instituto de Ciencia de Materiales, Aptdo. 1065, 41080 Sevilla, Spain*

Composites based on barium-containing cordierite glass-ceramic matrices reinforced with 20 and 30 vol% SiC platelets were fabricated by hot-pressing. The ceramed specimens were tested in compression at 1000, 1200 and 1300 °C in air, parallel and perpendicular to the hot-pressing direction. Compressive fracture stresses up to 460 MPa were recorded at 1000 °C. Lower stresses were observed at 1200 and 1300 °C. The compressive stress decreased with increase in the SiC platelet content and with the compressive direction being parallel to the hot-pressing axis. The mechanical behaviour at high temperatures was related to the presence of a residual glassy phase within the cordierite matrix, as well as to the mode of the crack nucleation within the composites.

## 1. Introduction

Glass-ceramics are among the advantageous oxide matrices for ceramic matrix composites (CMC) owing to their low-temperature fabrication, at which 100% relative density may be achieved. The cordierite-based (magnesium alumino-silicate; MAS) glass-ceramics are characterized by low coefficient of thermal expansion, which contributes to the geometrical stability at high temperatures, as well as to the improved thermal shock resistance. Nevertheless, the chemical compatibility between the oxide matrix and the non-oxide reinforcing component, has a major role in controlling the reinforcing effectiveness and the high-temperature deformation mechanism.

Recently, improvements both at room-temperature bending strength and fracture toughness were reported for cordierite glass-ceramics reinforced either with SiC whiskers, platelets, or fibres [1–6]. However, few data are available on the high-temperature deformation behaviour of these composites [3, 7]. A barium-doped cordierite matrix composite with 25 vol% SiC whiskers was reported to retain 60% of its room-temperature strength at 1200 °C. The present paper describes the high-temperature compression behaviour of SiC platelet-reinforced cordierite matrices.

## 2. Experimental procedure

Composites based on barium-containing cordierite glass-ceramic matrices reinforced with 20 and 30 vol% SiC platelets were fabricated (Table I). The mechanically mixed powders were cold pressed at 200 MPa into discs, followed by uniaxial hot pressing at 900 °C for 10 min in an argon atmosphere; the

applied pressure was 20 MPa, the heating rate 30 °C min<sup>-1</sup>. The fabrication procedure is described in detail elsewhere [5]. The relative densities of these composites were measured by the Archimedes' method to be 99.3% and 98.7%, respectively.

High-temperature compression tests were performed in air on parallelepipeds of 5 mm × 3 mm × 3 mm, at 1000, 1200 and 1300 °C, and a constant cross-head speed of 5 μm min<sup>-1</sup>. The compression direction was either parallel or perpendicular to the hot-pressing axis (Table II) using loading blocks of polycrystalline alumina. The specimens were heated at the rate of 50 °C min<sup>-1</sup> to the testing temperature, and preloaded under 3 kg load to keep the specimen in place. This preloading often caused a deformation of ~10% by viscous flow of the amorphous matrix. In order to avoid this deformation, the specimens were annealed for 2 h prior to the compression. The compression tests were stopped after ~30 min. Appropriate compositions were heat treated similarly without deformation as control specimens.

TABLE I Technical data for Ba-MAS matrix<sup>a</sup> and SiC platelets<sup>b</sup>

Chemical composition (wt %)		Physical properties
SiO <sub>2</sub>	52.5	Density = 2.65 g cm <sup>-3</sup>
Al <sub>2</sub> O <sub>3</sub>	32.0	T <sub>glass</sub> = 815 °C
MgO	13.5	T <sub>cryst</sub> = 1150 °C
BaO	2.0	
SiC-6H polytype		Diameter 50–250 μm Thickness 5–25 μm

<sup>a</sup> EG-0221, Ferro Corp., Cleveland, OH.

<sup>b</sup> American Matrix Inc., Knoxville, Tennessee, USA.

TABLE II MAS-SiC platelet composites deformed at high temperature

Specimen designation <sup>a</sup>	SiC (vol %)	Compression axis <sup>b</sup>	Compression temperature (°C)	Maximum stress (MPa)	Maximum strain (%)
1	20	⊥	1000	464	4.2
2	20	∥	1000	245	2.6
3	20	⊥	1200	247	3.6
4	20	⊥	1300	36	0.9
5	20	∥	1300	38	1.8
6	30	⊥	1200	214	3.6
7	30	⊥	1300	55	1.9

<sup>a</sup> See Fig. 1 for stress-strain curves.

<sup>b</sup> ∥ parallel, or ⊥ perpendicular, to the hot-pressing direction.

The microstructure of the specimens were examined before and after the deformation using transmission (TEM) and scanning (SEM) electron microscopy. The specimens for TEM and SEM were prepared by the conventional methods.

### 3. Results and discussion

The composite specimens were deformed to various strains, where only the 1300 °C experiments were stopped without fracture. Engineering stress-strain curves for seven different specimens (a-g in Table II) are shown in Fig. 1a and b for the 20% and 30% composites, respectively. The main features of these curves may be summarized as follows.

(i) At a given SiC content and deformation direction, the compressive stresses decrease significantly with increasing temperature.

(ii) At a given deformation temperature, the maximal stresses increase when the compressive direction is perpendicular to the hot-pressing axis.

(iii) The slope of the curves, which is indicative of the composite elastic modulus, decreases with increase of the deformation temperature.

Visual inspection indicated on the formation of a foam-like glassy layer at the free surfaces of the specimens tested at 1300 °C (Fig. 2a). This layer was absent in the specimens deformed at 1000 °C (Fig. 3a). The surface morphology of the specimens deformed at 1300 °C was composed of a glassy layer with many exploded bubbles and microcracks (arrowed in Fig. 2b). Traces of the dissolved SiC platelets were visible at the bottom of the bubbles (Fig. 2c). The specimens deformed at 1000 °C showed smoother surfaces (Fig. 3a) which contained very fine cavities (Fig. 3b). These surface morphologies were independent of the SiC content in the composites. Similar surface morphologies were observed in the respective control specimens. The interior microstructure of the specimens deformed at 1300 °C contained many cavities, aligned in bands within the glass-ceramic matrix (Fig. 4), relative to the dense nature of their undeformed counterparts.

TEM observations (Figs 5 and 6) revealed that the SiC platelets were mostly preserved at the interior of the specimens, irrespective of the deformation temperature. While in a 1000 °C specimens, a few amorphous-like defects were observed at the SiC/cordierite

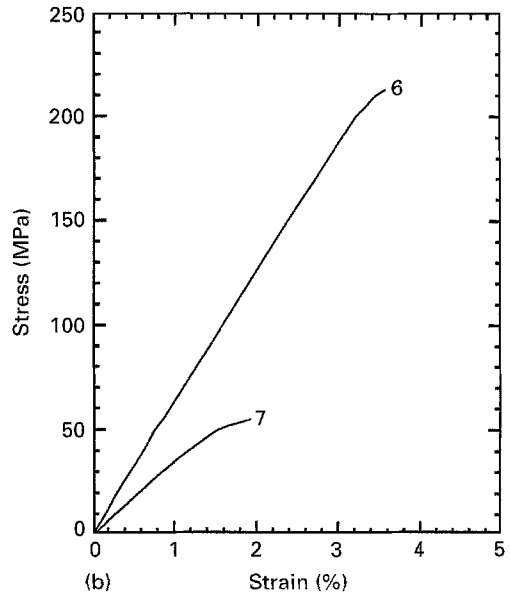
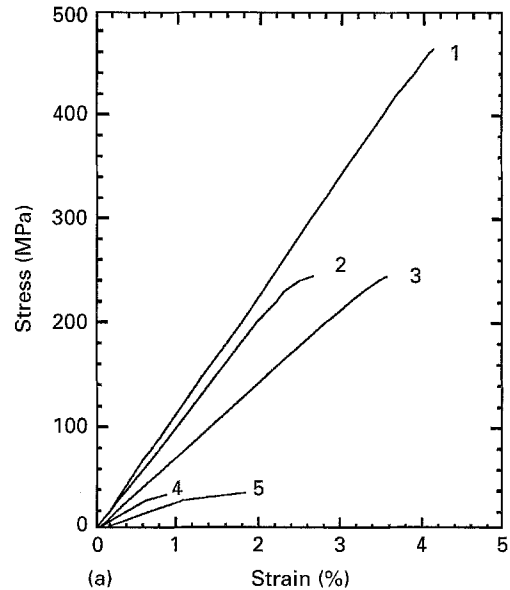


Figure 1 Engineering stress-strain curves of the BMAS/SiC platelet composites. (a) 20 vol % SiC, (b) 30 vol % SiC. See Table II for further details.

ous-like defects were observed at the SiC/cordierite interfaces (Fig. 5a), thicker and continuous amorphous layers were observed along all such interfaces in the 1300 °C specimens (Fig. 6a). In addition, in a

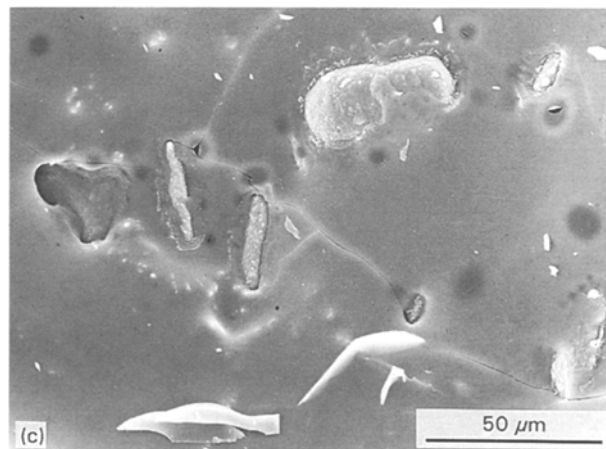
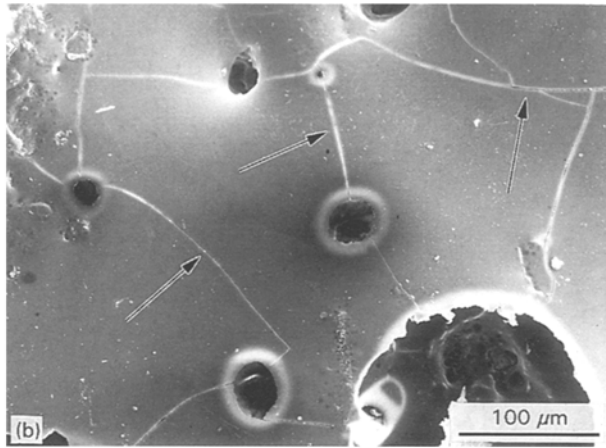
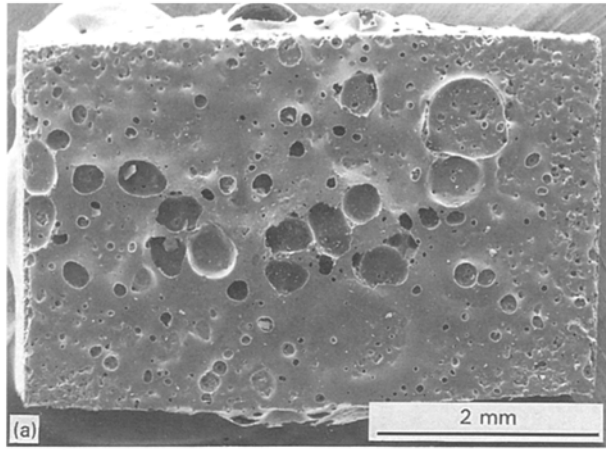


Figure 2 SEM images showing (a) the bubbled and (b) the microcracked glass layer at the surface of the MAS-20 % SiC specimen deformed at 1300 °C. (c) The traces of the dissolved SiC platelets are visible at the bottom of the bubbles.

1000 °C specimens, the cordierite matrix grains contained dislocations which were associated with amorphous precipitates (Fig. 5b), whereas in the 1300 °C specimens, the precipitates were finer and almost dislocation-free (Fig. 6b). These precipitates were proved by energy dispersive spectroscopic (EDS) analyses to be silica-rich.

The change in the deformation behaviour of the present composites should be related to the microstructural evolution within them at the different temperatures of concern. According to the crystallization

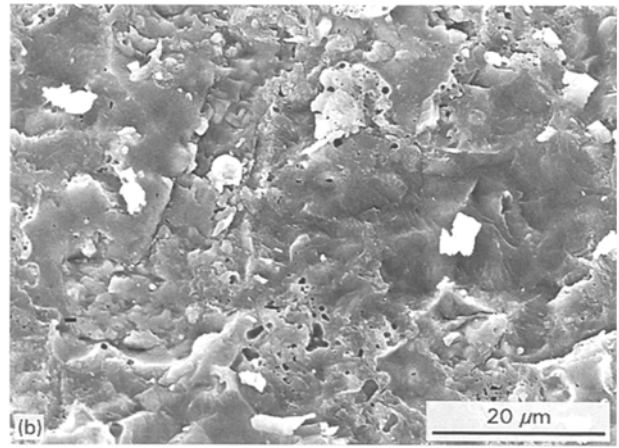
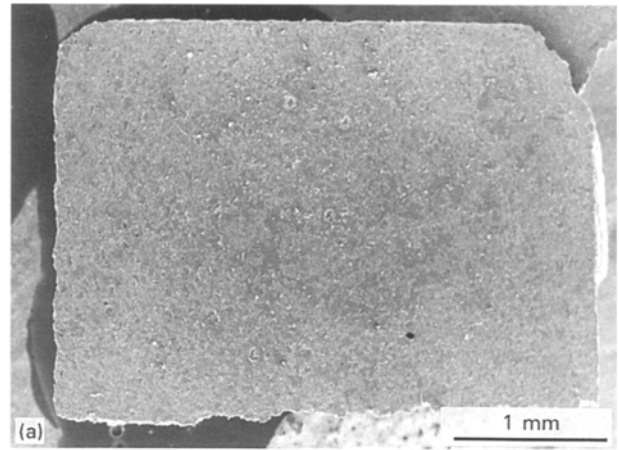


Figure 3 SEM images showing (a) the thermally etched surface of the MAS-30 % SiC specimen deformed at 1000 °C, and (b) traces of the dissolved SiC platelets visible on the surface.

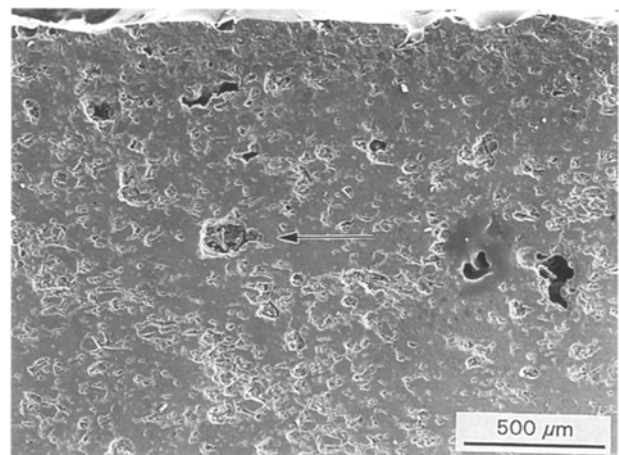


Figure 4 SEM image showing the cavities in specimen 7 aligned in bands (mid-left and mid-right to the bottom). The compression axis is shown by the arrow.

behaviour of the present barium-containing MAS [8], it is clear that the matrix was crystallized prior to the deformation. The crystallized and undeformed microstructure should contain relatively large dendritic cordierite crystals, which are associated with interdendrite barium-rich silicate glassy phase [8,9]. However, with respect to the TTT diagram for crystallization of this glass-ceramic [8], the 1300 °C specimens are expected to be fully crystallized while the

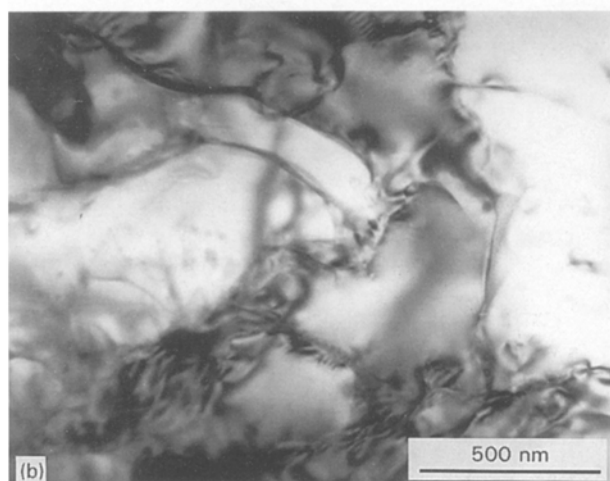
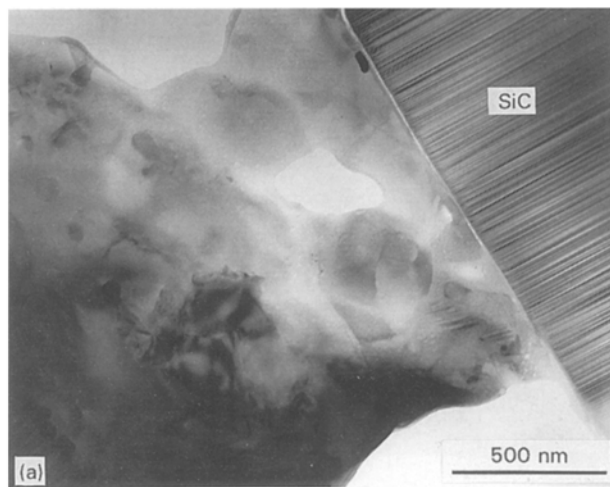


Figure 5 TEM image showing (a) amorphous-like defects at the SiC/cordierite interface, and (b) dislocations associated with precipitates within the cordierite grains. Specimen 2.

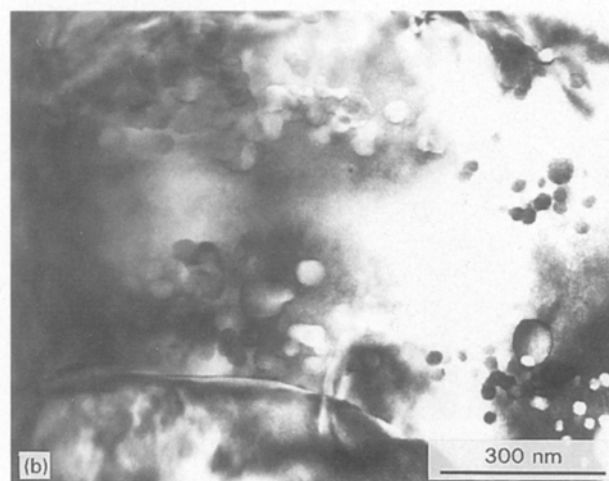
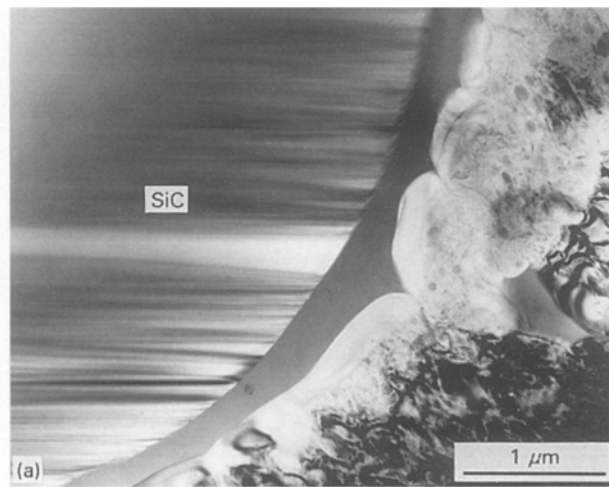
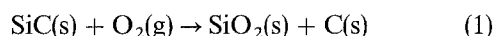


Figure 6 TEM image showing (a) the continuous amorphous layer at the SiC/cordierite interface, and (b) very fine dislocation-free precipitates within the cordierite grains. Specimen 6.

1000 °C specimens may contain some residual glassy phase.

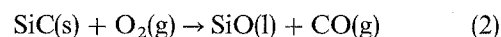
On the other hand, simultaneous oxidation of the SiC at the SiC/glass-ceramic interfaces should also be considered. According to the Ellingham diagram, oxidation of SiC at temperatures below 1150 °C and oxygen pressures above 1 torr (1 torr = 6.89 N mm<sup>-2</sup>) is in the passive mode [10,11], i.e. following the reaction



In such a regime, one may expect formation of a silica layer at the external surfaces of the specimen, where the supply of gaseous oxygen is unlimited. In addition, the resultant carbon most probably will be oxidized to gaseous CO. However, at the specimen interior, where the oxygen flow is diffusion-limited, formation of a carbon-rich layer is expected at the SiC/glass-ceramic interfaces, as was reported for different composite systems [9, 12–14].

With respect to the SiC oxidation reactions, SiO(l) is the only stable liquid which may be present between 1150 and 1350 °C. Thus, the bubble-like morphology of the surface glassy layer is a result of the CO bubbling within the viscous SiO liquid, according to the

following reaction



Such a bubble formation in the oxide scales was related to preferential oxidation of the carbon inclusions in polycrystalline SiC [15].

Although the evolution of surface morphology at 1000 and 1300 °C may be quite different, the diffusion-limited flow of oxygen across the SiC/glass-ceramic interface is expected to yield similar phase evolution in the specimen interior, namely formation of a carbon-rich layer at the SiC/cordierite interfaces. The only difference lies in the oxidation kinetics [10, 16, 17], which will lead to a more continuous and thicker carbon layer at the higher temperature.

The actual deformation temperatures are fairly high, from 0.73–0.90 of the cordierite melting point. At the lower temperature, the  $\sigma$ - $\epsilon$  curves indicate that the samples do not undergo plastic deformation, but failed in the elastic regime. The significant differences in the maximal stresses measured for the two different compression orientations should be related both to the elastic moduli and the load-bearing capacity of the composites.

The preferred orientation of the SiC platelets within the present hot-pressed specimens has been well

demonstrated [5]. The case for which a compression axis is perpendicular to the hot-pressing direction represents the upper bound for the elastic modulus of the composite. Thus, the composite strength is mainly determined by the strength of the harder component, i.e. SiC platelets. High elastic modulus and strength will also lead to high stresses to failure. On the other hand, the case for which a compression axis is parallel to the hot-pressing direction represents the lower bound for the elastic modulus of the composite. In this case, the composite strength is mainly determined by the strength of the weaker component, i.e. cordierite grains. Consequently, lower stresses may be expected at failure. Similar behaviour is expected both for tensile and compression tests.

Neglecting the residual stresses due to the thermal expansion mismatch between the cordierite grains and the SiC platelets at high temperatures, the SiC/cordierite interfaces become an important factor in geometrically determining the favourable sites for crack nucleation.

However, at 1300 °C, some plastic deformation is visible from the deformation curves. Viscous flow via SiO along the SiC/cordierite interfaces may be responsible for the plastic deformation. On the other hand, at 1000 °C (0.73  $T_m$ ), the cordierite matrix is expected to be more rigid with respect to the plastic deformation. Nevertheless, the residual amorphous regions within the matrix as well as at the SiC/matrix interfaces will contribute to the composite toughness by which relatively high strength may be expected [18, 19].

Similar trends of degradation in strength at high temperatures were reported in alumina reinforced with SiC whiskers [20], and related to the oxidation reactions and creep phenomena. Plastic deformation in the same composite was related to the diffusional flow at high SiC loadings, and to the grain-boundary sliding at lower SiC loadings [21]. Similarly, Gadkaree [3] has shown that the main reason for the substantial decrease in strength at high temperatures in SiC fibre/glass-ceramic composites is the change in the load-transfer mechanism, i.e. from the elastic-elastic to elastic-plastic regime. This occurred mainly due to the sudden decrease in the shear modulus of the SiC/cordierite composite above 1000 °C.

Generally, cavity nucleation should be associated with tensile stresses. However, in compression tests, such tensile stresses may be developed locally by grain-boundary sliding via the amorphous grain-boundary phase. The formation of the cavities in large bands is indicative of the shear process, most probably occurring by viscous flow along the SiC/cordierite

interfaces. Compression tests of anorthite glass-ceramic at high temperatures [22] exhibited a similar type of cavitation and viscous flow.

Finally, because extensive cavitation occurred within the compressed composites at ~4% strains, lower plastic strains may be expected for tensile conditions.

## Acknowledgements

The Sachs Centre at the Department of Materials Engineering is acknowledged. This research was supported by the Fund for the Promotion of Research at the Technion. R. Chaim thanks D. Sherman for fruitful discussions. In Seville, the research was supported by CICYT MAT 91-0978.

## References

1. I. WADSWORTH and R. STEVENS, *J. Mater. Sci.* **26** (1991) 6800.
2. *Idem*, *J. Eur. Ceram. Soc.* **9** (1992) 153.
3. K. P. GADKAREE, *J. Mater. Sci.* **26** (1991) 4845.
4. L. R. DHARANI, M. N. RAHAMAN and S-H. WANG, *ibid.* **26** (1991) 655.
5. R. CHAIM and V. TALANKER, *J. Am. Ceram. Soc.* **78** (1995) 166.
6. K. P. GADKAREE and K. CHYUNG, *Am. Ceram. Soc. Bull.* **65** (1986) 370.
7. S. M. BLEAY and V. D. SCOTT, *J. Mater. Sci.* **27** (1992) 825.
8. R. CHAIM and A. H. HEUER, *J. Am. Ceram. Soc.* **75** (1992) 1512.
9. *Idem*, *ibid.* **74** (1991) 1663.
10. S. C. SINGHAL, *J. Mater. Sci.* **11** (1976) 1246.
11. A. H. HEUER and V. L. K. LOU, *J. Am. Ceram. Soc.* **73** (1990) 2785.
12. J. J. BRENNAN and S. R. NUT, *ibid.* **75** (1992) 1205.
13. R. CHAIM and A. H. HEUER, *Adv. Ceram. Mater.* **2** (1987) 154.
14. R. F. COOPER and K. CHYUNG, *J. Mater. Sci.* **22** (1987) 3148.
15. D. M. MIESKOWSKI, T. E. MITCHELL and A. H. HEUER, *J. Am. Ceram. Soc.* **67** (1984) C-17.
16. J. A. CASTELLO and R. E. TRESSLER, *ibid.* **64** (1981) 327.
17. R. C. A. HARRIS, *ibid.* **58** (1975) 7.
18. S. M. WIEDERHORN, B. J. HOCKEY, R. F. KRAUSE Jr and K. JAKUS, *J. Mater. Sci.* **21** (1986) 810.
19. A. G. EVANS and B. J. DALGLEISH, *Ceram. Eng. Sci. Proc.* **9-10** (1986) 1073.
20. P. F. BECHER and T. N. TIEGS, *Adv. Ceram. Mater.* **3** (1988) 148.
21. A. R. DE ARELLANO-LOPEZ, A. DOMINGUEZ-RODRIGUEZ, K. C. GORETTA and J. L. RUTBORT, *J. Am. Ceram. Soc.* **76** (1993) 1425.
22. R. F. MERCER and A. H. CHOKSHI, *Scripta Metall. Mater.* **28** (1993) 1177.

Received 14 April 1994

and accepted 4 October 1995